Initial-stage oxidation mechanism of Ge(100)2×1 dimers

Jia Mei Soon, Chee Wei Lim, and Kian Ping Loh*
Department of Chemistry, National University of Singapore, 3 Science Drive 3, 117543 Singapore

Ngai Ling Ma and Ping Wu
Institute of High Performance Computing, 1 Science Park Road, The Capricorn, Singapore Science Park II, 117528 Singapore
(Received 6 June 2005; published 29 September 2005)

The initial stage oxygenation of the Ge(100) surfaces has been studied using density functional theory and high resolution electron energy loss spectroscopy. The sequences of the addition of dissociated O_2 on the Ge-Ge bridged and backbonded sites were considered in order to correlate the energetics of the reactions predicted by first principles calculations with the surface vibrational modes observed in our experiments. Our results suggest that a one O_2-per-dimer site reaction is more favorable than the dissociative chemisorption of O_2 across two dimer sites. The first insertion of one O into the Ge backbond is apparently barrierless; further thermal activation allows the second O bridging the dimer site to be inserted into the second Ge backbond in the same dimer.

DOI: 10.1103/PhysRevB.72.115343 PACS number(s): 68.43.−h, 79.20.Uv, 68.47.Fg, 68.43.Pq

I. INTRODUCTION

Despite having high carrier mobility and the availability of crystals of high purity, germanium (Ge) semiconductors have been overshadowed in the past by silicon because of the instability of its oxide. Ge does not have a stable, defect-free and abrupt oxide interface needed for gate applications in the metal-oxide-semiconductor-(MOS) based transistor technology. Nevertheless, Ge remains an attractive candidate for the manufacture of metals insulator semiconductor (MIS) devices.[1] In addition Si-Ge heterostructures are now defining the performance of gate structures in new-generation transistor devices.[2,3] Recently, it has been demonstrated that MOS capacitors (MOS-C) and field-effect transistors (FET) can be made by the deposition of ultrathin zirconium oxide on the Ge substrate.[4,5] The surface oxidation of Ge at the interface will affect the performance of any forms of devices based on Ge. While the oxidation mechanism of Si has been intensively researched in the last twenty years, there have been very limited studies on the surface oxidation of Ge.[6–10] The preparation of a clean and atomically flat Ge(100)2×1 using UV-generated ozone has been reported by Hovis and co-workers.[11] Using high resolution x-ray photoelectron spectroscopy, Tabet and co-workers[12] showed the presence of high density of electronic states located at the GeO_2/Ge interface. The detailed mechanism of how O_2 form the initial oxidation products on Ge is not known, although analogous chemistry with that of silicon could be expected due to the structural similarity between the two.

The spontaneous dissociative chemisorption of O_2 on silicon surfaces has been the subject of several experimental and theoretical studies.[13,14] The tilted dimer geometry on the silicon(100)2×1 surface facilitates electron transfer from the up-dimer atom to the antibonding orbital of oxygen molecule, in the process weakening the molecular bonds in O_2 and resulting in its dissociative chemisorption.[15] The essential features of the initial oxidation processes are summarized as: (i) the existence of channels for almost barrierless dissociative chemisorption, (ii) an inclination towards backbond oxidation. Watanabe *et al.* obtained strong evidence that the backbond oxidation of Si(100) surface proceeds with almost no activation barrier. The enhanced buckling of Si dimers after oxidation observed by scanning tunnel microscopy (STM) measurement also suggests backbond oxidation.

The dimer bonds on Ge(100)2×1 are more polar than that of silicon and enjoy a greater degree of buckling.[16,17] It is reasonable to deduce that the dissociative chemisorption of O_2 on Ge should, similar to silicon, proceed spontaneously, with backbond oxidation as the stable product. Using STM, Fukuda[8,29,30] observed that dimer buckling is stablilized after the initial stage oxidation. This could be due to the insertion of O into the Ge backbonds. However, their conclusions based on the interpretations of the STM images is in contradiction with the trend commonly interpreted for silicon. They ascribed backbonded configuration as metastable products formed at the initial stage, while the bridged site configuration as the stable product at higher temperature. Their report suggests that the oxidation mechanism on silicon should be opened to re-interpretation considering the structural similarity between Si and Ge. Clearly the reaction mechanism for the initial stage oxidation of Ge (100) is an open-ended question. The interpretation of STM images is not straightforward because of the changes in local density of states with the attachment of oxygen, as well as possible adsorption on defect sites. Motivated thus, we performed the high resolution electron energy loss spectroscopy (HREELS) study of the initial stages following the adsorption of O_2 on the Ge surface at room temperature. The HREELS technique can probe directly the chemical bonding configurations of oxygen on the Ge surface during the various stages of reaction.

II. EXPERIMENTAL

The experiments took place in a dual-chamber UHV system. The analysis section is equipped with a mu-metal shielded Delta 0.5 HREELS spectrometer (SPECS GmbH)

 ©2005 The American Physical Society

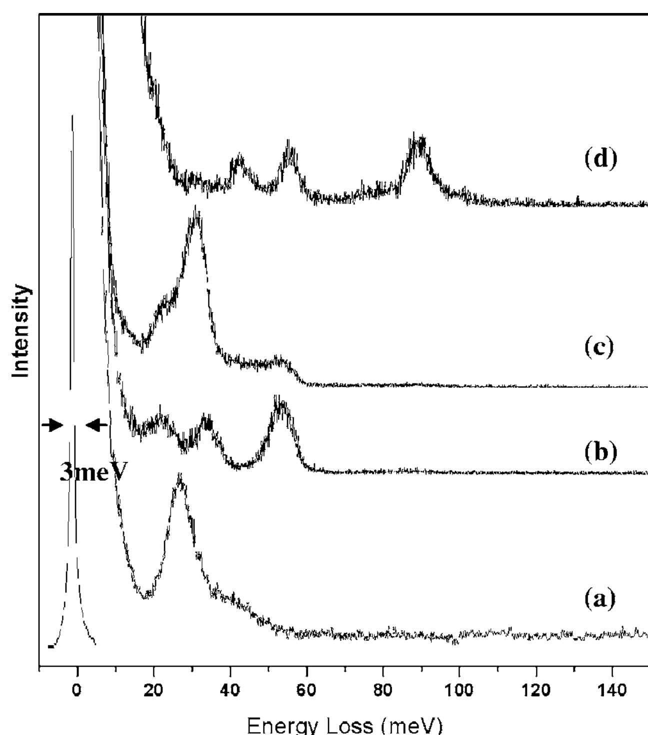

FIG. 1. HREELS spectra of the (a) clean Ge(100)2×1 surface with the surface phonon mode at ∼28-35 meV, (b) after dosing 12 L of O_2 at room temperature, (c) after annealing to 50 °C, and (d) after annealing to 100 °C.

and a reflection high energy electron diffraction (RHEED) system. In the sample preparation section, argon sputtering and gas dosing facilities are available. The base pressure of the system is 1×10^{-10} Torr. The sample used was an *n*-doped (5.3×10^{17} Sb) Ge(100). The sample was subjected to multiple cycles of argon sputtering (600 eV) and flash annealing to 600 °C until a clear 2×1 pattern emerged in the RHEED pattern. For the oxygen dosing experiment, ultrapure oxygen gas was leaked in through a precision leak valve. For all the HREELS data, an incident electron energy of 5.0 eV was used and the full width at half maximum (FWHM) of the specular peak during measurement on the clean surface was adjusted to 3 meV. A clean surface is characterized by the appearance of a sharp 2×1 reconstruction pattern in RHEED, as well as the presence of a surface phonon peak at about 28 meV as shown in Fig. 1(a). Details on these have already been described elsewhere.[10]

III. THEORETICAL CALCULATIONS

In this work, a Ge_9H_{12} cluster is used to model the Ge(100)2×1 surface for all energy minimum calculations. The dangling bonds on the clusters are terminated with hydrogen atoms. All atoms in the cluster model are allowed to relax fully using the B3LYP hybrid gradient-corrected density functional theory (DFT) method with Becke's exchange functional[18] and the Lee-Yang-Parr[19] correlation. The electronic structure is expanded using polarization basis functions of 6-31$G(d)$ developed by Petersson and co-workers[20,21] in the GAUSSIAN98 suite.[22] The calculated infrared (IR) frequency data are scaled by a correction factor of 0.9806, in accordance to previous work done by Scott and Radom.[23] The buckling angle (∼16°) of the dimer for this optimized cluster model is in good agreement with previous calculations based on the periodic slab.[24–26]

For the calculation of transition states, we use the Hatree-Fock (HF) method with a basis set of 6-31$G(d)$ for greater computational efficiency. To consider the interdimer mechanism, we employ a larger cluster, $Ge_{17}H_{20}$ to model two neighboring dimers sites, in order to account for any lateral interaction effects. In this work, the calculation of all transition states was performed with no constrained degree of freedom. All transition states reported in this paper are checked to have exactly one imaginary frequency. A transition state structure linking two minima on a potential energy surface is characterized by a first-order saddle point which is a maximum in exactly one direction and a minimum in all other orthogonal directions. The finite displacement calculation is used to verify that the first-order saddle point is connecting two minima belonging to the reactant and product of interest.

IV. RESULTS AND DISCUSSION

Figure 1 shows the HREELS spectra of the Ge surface, starting from the bare Ge surface exhibiting phonon peak intensities stretching between ∼28-35 meV in Fig. 1(a), to spectra obtained after reacting with molecular oxygen at room temperature [Fig 1(b)], followed by annealing to 50 °C and 100 °C, respectively [Figs. 1(c) and 1(d)]. The peak intensities of the phonon modes shown in Fig. 1(a) are within the frequency regions predicted by previous theoretical calculations of the Ge surface dimer vibrational modes.[27] It is well established by experiments[28] that Si has an optical loss peak at 56 meV; simple extrapolation based on reduced mass calculation (the ratio of the square root of the Ge and Si masses ∼1.61) predict that the analogous loss mode in Ge will be around 34 meV. This simple prediction agrees remarkably well with the theoretical phonon density of state calculation by Tutuncu *et al.*[27] using the adiabatic bond charge model, where the major phonon peak was calculated to be at 35 meV. Our own DFT calculations using the Ge dimer model shows dimer stretching mode to be located at 35 meV. In actual conditions, the position of this surface phonon peak is sensitive to the sample preparation conditions due to phonon-plasmon coupling on doped surfaces.[8]

Following exposure to 12 L [1 langmuir (L) $=1\times10^{-6}$ Torrs] of O_2, three distinct peaks at 22 meV, 34 meV, and 54 meV appear in the HREELS spectra in Fig. 1(b). When the same sample was annealed to 50 °C, there is a dramatic increase in a vibrational peak signal at 31 meV in Fig. 1(c). There is also a shoulder at 22 meV and a peak at 54 meV. After a further annealing of the same sample to 100 °C, two new peaks appear at 43 meV and 89 meV in Fig 1(d). Clearly, the chemisorption configurations of oxygen are changing at each thermal activation step. If the sample was exposed to higher dosages of oxygen at 1000 L and higher, the elastic peak rapidly broadened and the fine features became lost in the inelastic tail, and peaks associated

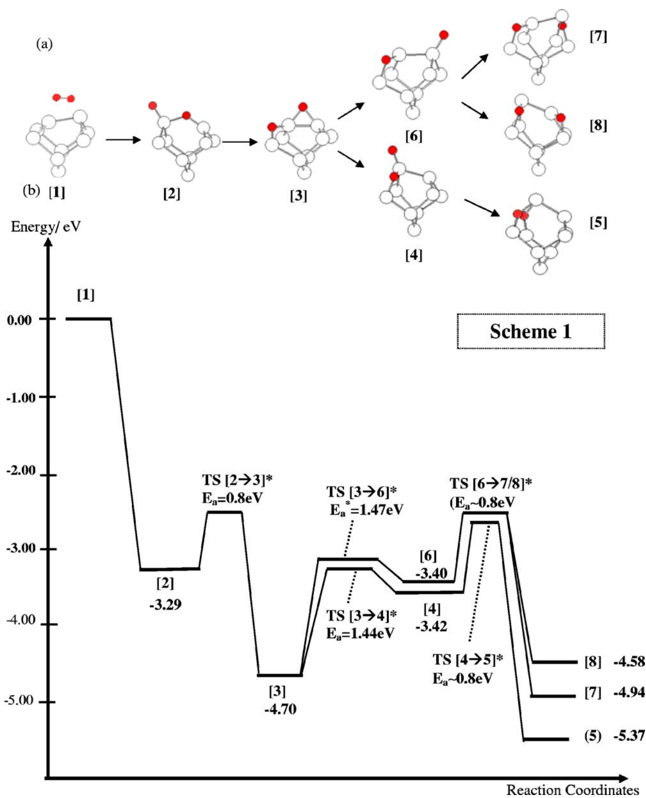

FIG. 2. (a) (Color online) Schematic diagram of possible products and (b) the associated energetics following the dissociative chemisorption of oxygen molecule on the Ge dimer, as outlined in Scheme 1.

with bulk oxidized Ge-O-Ge modes appeared. These bulk oxidized modes have been previously reported[8] so we will not discuss these, and instead we focus our attention here on the initial oxygen chemisorption stages involving the dimers on the Ge(100)2×1 surface.

Assuming that O_2 undergoes spontaneous dissociative chemisorption on the Ge dimer sites at room temperature, we consider two possibilities for the initial adsorption configuration. Figure 2 shows the schematic for the intradimer mechanism, in which one O_2 attacks a dimer site, and following the dissociation of the O_2, a bridging O bonds on top of the dimer, and a backbonded O inserts in the same dimer, forming structure [3]. The associated transition state energy level diagrams are shown below the schematic drawing. To go from structure [1] to [3], we propose that it will go through an intermediate state [2]. We have identified the transition state and an activation barrier of 0.8 eV before [2] can be converted into [3]. Due to the exothermicity of the reaction going from [1] to [2], the energy release of −3.29 eV per O_2 molecule helps to overcome the activation barrier and transfers the system to [3], so the reaction is effectively barrierless. The overall enthalpy change to produce [3] from [1] is −4.70 eV per O_2 molecule. Going from [3] to a doubly backbonded structure like [5], [7], or [8] will require going through metastable states [4] or [6] and the reaction is endothermic. In addition, two activation barriers exist in the path. The activation barriers for [3] to go to [4] or [6] are 1.44 eV and 1.47 eV respectively, and for [4] or [6] to go to [5], [7], or [8] is ∼0.80 eV. Therefore on both kinetic and thermodynamic grounds, the reverse reaction to generate [3] from [4] or [6] is more favorable than the forward reaction. Therefore in the absence of energy input, we expect that [3] will be the most stable structure at low temperature, because thermal activation is needed in order to surmount the energy barriers for reaching the doubly O-backbonded structures [5], [7], or [8]. The overall enthalpy change referenced to the clean surface [1] is −5.37 eV per O_2 molecule for forming structure [5].

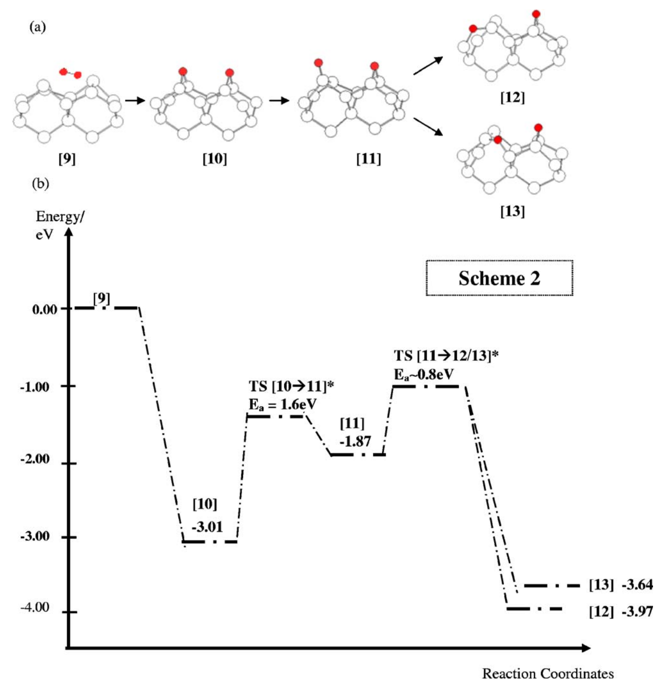

FIG. 3. (a) (Color online) Schematic diagram of possible products and (b) the associated energetics following the dissociative chemisorption of oxygen molecule on the Ge dimer pairs, as outlined in Scheme 2.

Figure 3 shows the reaction schematic for the interdimer mechanism, together with the associated transition state energy levels. In this case one O_2 dissociates across two neighboring dimer sites to produce two bridged Os on top of the two dimers, forming structure [10]. To convert [10] to a structure with one O in the backbonds, i.e., structure [12] and [13], will require going through a metastable state [11]. This is because one of the bridging O bonds on the dimer has to be first broken and a dangling bond generated before the subsequent insertion steps into the backbond can proceed. An activation barrier of 1.6 eV has to be overcome going from [10] to [11], and the reaction is endothermic. Further energy input for overcoming a second energy barrier of 0.8 eV is required to transfer the metastable state [11] into the more stable structure [12]. In this case the overall reaction is exothermic by −3.97 eV per O_2 referenced to the initial clean structure [9]. However, there is a kinetic and thermodynamic driving force for the metastable state [11] to slip back into the more stable structure [10] because the reverse reaction is exothermic and the activation barrier for the reverse reaction is smaller. Therefore in the absence of thermal activation, it can be expected that [10] is the more probable configuration adopted in this scheme.

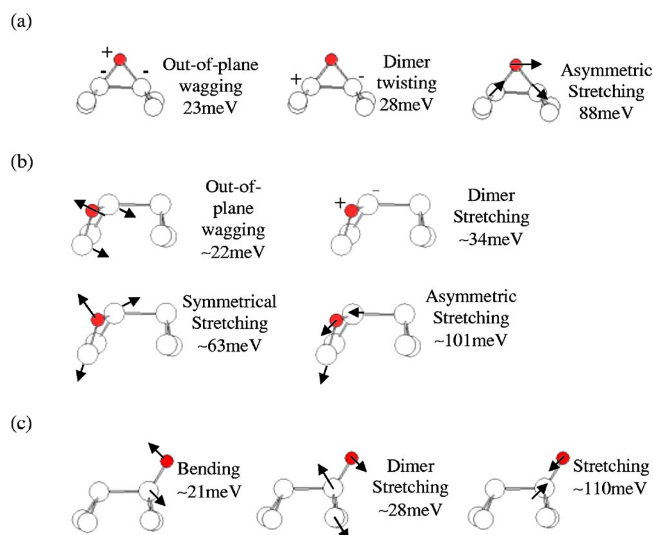

FIG. 4. (Color online) Characteristic vibration modes for (a) O-bridged dimer, (b) backbonded Ge—O—Ge, and (c) dangling Ge—O bond.

The above transition state calculations allow us to predict the stable configurations which occur at low temperature before thermal activation is applied. In the intradimer mechanism, structure [3], the configuration with one backbonded O and one bridged O in the same dimer, is predicted to be more stable because the large energy gain going from the clean surface structure to [3] helps to overcome the initial potential barrier. In the interdimer mechanism, structure [10], where both O atoms adopt the bridging sites on top of the dimer, is predicted to be the stable structure adopted at the initial stage of the oxygenation. Due to the strong Ge-O-Ge bond, considerable activation barriers have to be overcome before conversion into a backbonded structure.

A frequency analysis of the characteristic vibrational modes of the various structures is listed in Fig. 4. Figure 4(a) shows that the O-bridged dimer has characteristic vibrational modes at 23, 28, and 88 meV due to dimer bridge-related bending and stretching modes. Figure 4(b) highlights the characteristic backbond stretch at ~63 meV for Ge-O-Ge backbonded structure. Figure 4(c) shows a dangling Ge-O bond which can be generated from the breakage of the Ge-O-Ge bridged bonds, the Ge-O bending and stretching modes occur at 21 and 28 meV, respectively. In the original clean surface dimer mode, a rocking mode was observed at 14 meV and a stretch mode at 36 meV. Once O atoms are inserted into the backbonds to form the Ge-O-Ge backbond modes as in structure [5], the dimer stretching mode vanished, and only a weak twisting mode occurs at 30 meV. Therefore the trend suggests that following the backbond oxidation of the dimer, the original Ge-Ge dimer stretching mode at the low frequency regions will vanish, to be replaced by Ge-O-Ge backbond stretching modes at higher frequencies.

Table I shows the matching between the experimental HREELS signal and the characteristic vibrations of the theoretical models [1], [3], [4] and [5] used in this work. It is clear that the profiles of the experimentally observed vibrational peaks for the room-temperature oxidized Ge in Figure 1(b) are closer to the vibration modes of structure [3]. This is supported by the observation of the backbond vibrational modes at 54 meV, and also by the good agreement with dimer-bridge wagging and stretching modes at 22 and 34 meV. A strong enhancement in the HREELS peak at 30 meV was observed after annealing the oxidized Ge to 50 °C, as shown in Fig. 1(c). The origins for the strong enhancement of the peak at 30 meV is not clear, it could be due to the Ge-O dangling bonds generated on the dimer surface after partial disordering of the surface following slight

TABLE I. Peak matching between experimental HREELS signals and the characteristic vibrations modes of theoretical models [1], [3], [4], and [5]. These structures exhibit the smallest root-mean-square differences compared to the experimental results.

Experimental			Theoretical	RMS difference
Spectrum	Peak position (meV)	Structure	Peak position (meV)	Peak position (meV)
Clean	35	[1]	14 (dimer rocking)	
Surface			36 (dimer stretching)	1
30 °C	22	[3]	22 (bridge wagging)	
	34		34 (dimer stretching)	5.2
	54		63 (backbond stretching)	
50 °C	22	[4]	21 (dangling Ge-O bending)	
	31		31 (dimer and Ge-O stretching)	4.1
	54		61 (backbond symmetrical stretching)	
100 °C	43	[5]	39 (backbond wagging)	
	56		51 (backbond symmetrical stretching)	3.7
	89		88 (backbond asymmetrical stretching)	

thermal annealing. Free-dangling Ge-O bonds oriented vertical to the surface are strongly dipole active; therefore, the HREELS signals of these will be strong in the specular scattering mode. Our calculations show for example that a Ge-O dangling bond on the dimer has bending and stretching modes at 21 and 28 meV, respectively; these values are close to what we have observed at this stage. When the oxygenated Ge surface was further annealed to 100 °C, three peaks are observed at 43, 56, and 89 meV in Fig. 1(d) which agrees well with the characteristic vibrational profiles of the Ge-O-Ge backbonds in the doubly oxidized Ge dimer. Our calculations show that the characteristic Ge-O-Ge backbond vibration modes for structure [5] occur at 39 meV (wagging), 51 meV (symmetric stretch), and 88 (asymmetric stretch) meV, which agree well with the HREELS peaks in Fig. 1(d). Moreover, the vibrational frequencies of structure [5] show better agreement to the experimental spectrum in Fig. 1(d), compared to structures [7] and [8].

Our results suggest that during the initial stages of oxygenation of Ge, several distinct chemisorption states can exist between room temperature to 100 °C. These results agree with previous STM observations by Fukuda and co-workers[29,30] who observed several kinds of ordered structures consisting of Ge-O species in their combined photoemission spectroscopy and STM studies. They suggested that adsorbed O atoms can initiate ordered structures without roughening the Ge(100) surface. The evolution of the HREELS profile we have obtained here agree reasonably well with the sequences in the intradimer mechanism proposed by us. At room temperature, oxygen molecule dissociatively chemisorbs on the dimer to form a bridged O atom and backbonded O atom within the same dimer, i.e., structure [3]. Structure [3] acts as a precursor state that favors the further insertion of oxygen into the backbonds by lowering the activation barrier for insertion to about 1.44 eV, compared to the 1.6 eV required for the formation of [11]. Further annealing provides the impetus to insert the second bridged O into the Ge backbonds to form structure [5]. In the intradimer mechanism, there are three possible products following the insertion of the second O atom into the backbonds, depending on whether the Ge-O-Ge backbonds are on the same side of the dimer (structure [5]), or on the opposite side of the dimer, and whether they are in staggered (structure [7]) or parallel configuration (structure [8]). Reaction enthalpies show that [1]→[5] is energetically more favorable than [1]→[7] or [1]→[8]. Due to the insertion of two O atoms on the same side of the dimer for structure [5], the degree of tilting of the dimer, measured in terms of the vertical distance between the up dimer atom and down dimer atom, Δz, is 1.72 angstroms compared to 1.02 angstroms of the clean surface dimer. The Ge-Ge dimer bond distance has also expanded by 15% relative to the clean surface. On the clean surface, charge separation across the dimer atoms generates strong ionic bonding. After insertion of O atoms, redistribution of charges towards the electronegative O atoms weakens the dimer bond. Compared to structures [7] and [8], structure [5] is more stable. Mulliken charge analysis shows that insertion of O into the opposite side of the dimer in structures [7] and [8] will impart a partial positive charge on both the Ge dimer atoms due to the electron-withdrawing effect of O atoms. This can be prevented if the two Ge-O-Ge backbonds exist on the same side of the dimer, as in structure [5]. In addition, considerable strain occurs in [7] and [8] because of the need to accommodate different Ge-Ge and Ge-O-Ge bond distances in the backbonds. In an unstrained $H_8Ge_8O_{12}$ cluster,[10] the Ge-O-Ge bond angle is ~133°. In [7] and [8], the corresponding bond angles are compressed to ~116° and ~125°, respectively, in order to accommodate the dissimilar Ge-Ge and Ge-O-Ge bond lengths on the same side of the dimer. In structure [5], because the Ge-O-Ge backbonds and the Ge-Ge bonds occur on opposite sides of the dimer, the strain due to unequal bond lengths can be relieved by a higher degree of dimer tilting. This dimer tilting may be responsible for the previously observed bright spots in the STM following initial stage oxygenation.[8]

V. CONCLUSION

We have applied both HREELS and transition state calculations to study the initial stage oxidation mechanism of Ge dimers on the Ge(100)2×1 surface. The HREELS data show changes in the profiles of the vibrational peaks when the oxygenated Ge substrate was annealed to different temperatures, which indicate changes in the chemisorption configuration of O on the Ge surface. Our transition state calculations suggest that at the initial adsorption stage, the stable structure consists of one inserted oxygen atom in the Ge backbonds, and another oxygen atom occupying the bridging position between the Ge dimer atoms. Comparison of the energy barriers between the intradimer and interdimer mechanisms suggests that the intradimer mechanism is energetically more favorable. Considerable activation barrier has to be overcome before the bridging oxygen atom can be inserted into the backbonds. The HREELS spectrum of O-chemisorbed Ge structure annealed to 100 °C showed vibrational peaks that agree well with the model of the Ge dimer structure with two O atoms in the backbonds.

*Author to whom correspondence should be addressed. Electronic address: chmlohkp@nus.edu.sg

[1] L. Chun-rong and L. Ling, J. Phys. D **22**, 1169 (1999).
[2] D. L. Harame, J. H. Comfort, and J. D. Cressler, IEEE Trans. Electron Devices **42**, 455 (1995).
[3] D. L. Harame, J. H. Comfort, and J. D. Cressler, IEEE Trans. Electron Devices **42**, 469 (1995).
[4] C. O. Chui, S. Ramanathan, B. B. Triplett, P. C. McIntyre, and K. C. Saraswat, IEEE Electron Device Lett. **23**, 473 (2002).
[5] H. Shang, H. Okorn-Schimdt, J. Ott, P. Kozlowski, S. Steen, E. C. Jones, H. S. P. Wong, and W. Hanesch, IEEE Electron Device Lett. **24**, 242 (2003).

[6] E. J. J. Kirchner and E. J. Baerends, Surf. Sci. **311**, 126 (1994).
[7] K. Prabhakaran and T. Ogino, Surf. Sci. **325**, 263 (1995).
[8] T. Fukuda and T. Ogino, Phys. Rev. B **56**, 13190 (1997).
[9] C. Mui, J. P. Senosiain, and C. B. Musgrave, Langmuir **20**, 7604 (2004).
[10] C. W. Lim, J. M. Soon, N. L. Ma, W. Chen, and K. P. Loh, Surf. Sci. **575**, 51 (2005).
[11] Jennifer S. Hovis, Robert J. Hamers, and C. Michael Greenlief, Surf. Sci. **440**, L815 (1999).
[12] N. Tabet, M. Faiz, N. M. Hamdan, and Z. Hussain, Surf. Sci. **523**, 68 (2003).
[13] Akitaka Yoshigoe and Yuden Teraoka, Surf. Sci. **532–535**, 690 (2003).
[14] J. A. Schaefer, F. Stucki, D. J. Frankel, W. Gopel, and G. L. Lapeyre, J. Vac. Sci. Technol. B **2**(3), 359 (1984).
[15] Y. Miyamoto and A. Oshiyama, Phys. Rev. B **43**, 9287 (1999).
[16] S. J. Jenkins and G. P. Srivastava, J. Phys.: Condens. Matter **8**, 6641 (1996).
[17] D. J. Chadi, Phys. Rev. Lett. **43**, 43 (1979).
[18] A. D. Becke, J. Chem. Phys. **98**, 1372 (1993).
[19] C. T. Lee, W. Yang, and R. G. Parr, Phys. Rev. B **37**, 785 (1988).
[20] G. A. Petersson and M. A. Al-Laham, J. Chem. Phys. **94**, 6081 (1991).
[21] G. A. Petersson, A. Bennett, T. G. Tensfeldt, M. A. Al-Laham, W. A. Shirley, and J. Mantzaris, J. Chem. Phys. **89**, 2193 (1988).
[22] M. J. Frisch, G. W. Trucks, H. B. Schlegel *et al.*, GAUSSIAN 98, Gaussian, Inc., Pittsburgh, PA, 1998.
[23] Anthony P. Scott and Leo Radom, J. Chem. Phys. **100**, 16502—16513 (1996).
[24] P. Kruger and J. Pollmann, Phys. Rev. Lett. **74**, 1155 (1994).
[25] A. Pasquarello, M. S. Hybertsen, and R. Car, Phys. Rev. B **54**, R2339 (1996).
[26] K. S. Schneider, Z. Zhang, M. M. Banaszak, B. G. Orr, and U. C. Pernisz, Phys. Rev. Lett. **85**, 602 (2000).
[27] H. M. Tutuncu, S. J. Jenkins, and G. P. Srivastava, Phys. Rev. B **57**, 4649 (1998).
[28] H. Ibach, Phys. Rev. Lett. **27**, 253 (1971).
[29] T. Fukuda and T. Ogino, Appl. Surf. Sci. **130**, 165 (1998).
[30] T. Fukuda, Jpn. J. Appl. Phys., Part 2 **38**, L1450 (1999).